Coati Optimization based ANFIS MPPT for PV-Battery Integrated System to Improve Power Quality

Nirmal Kumar Pandey[1], Rupendra Kumar Pachauri[2,3,*]

[1]Department of Electronics & Communication, Shivalik College of Engineering, Dehradun-248197, India
[2]Electrical Cluster, School of Advanced Engineering, University of Petroleum & Energy Studies, Dehradun-248007, India
[3]Miyan Research Institute, International University of Business, Agriculture and Technology, Dhaka-2030, Bangladesh

*Author to whom correspondence should be addressed:
E-mail: nirmalpande84@gmail.com (NKP); rpachauri@ddn.upes.ac.in (RKP)

(Received January 26, 2025; Revised September 18, 2025; Accepted October 28, 2025)

Abstract: This research presents an innovative method to improve photovoltaic (PV) systems integrated with batteries, emphasizing efficient power extraction and enhanced power quality. It combines the Coati optimization algorithm, inspired by coati foraging behaviour, with Adaptive Neuro Fuzzy Inference Scheme (ANFIS) for precise maximum power point tracking (MPPT) under fluctuating solar conditions. The Coati algorithm ensures optimal energy harvesting, while battery storage mitigates solar energy intermittency. The system also addresses power quality challenges, reducing harmonic distortion and improving voltage stability. With an efficiency of 99.3% under standard test conditions, a settling time of 0.11 seconds, a THD value of 0.58%, RMSE values of 1.4842e-13, and a mean error of 5.789e-14, simulations show that it outperforms conventional MPPT methods, promoting the development of efficient, dependable, and sustainable PV-battery systems for contemporary power grids.

Keywords: Coati algorithm; Maximum Power point; Power quality; PV system.

1. Introduction

The increasing worldwide need for sustainable energy sources has driven extensive research into photovoltaic (PV) systems, providing a viable solution for electricity generation. However, the inherent variability of solar energy production necessitates advanced technologies to optimize energy extraction. MPPT algorithms are crucial for optimizing the efficiency of PV systems as they dynamically fine-tune operational parameters to harness the utmost power from solar panels. In this study, we introduce an innovative approach that combines the Coati optimization algorithm with the Adaptive Neuro Fuzzy Inference Scheme (ANFIS) to enhance MPPT in PV systems. The Coati algorithm draws inspiration from the cooperative foraging behavior of coatis, offering a unique optimization strategy to improve the tracking accuracy and efficiency of ANFIS, ultimately enhancing energy harvesting capabilities.

Moreover, the integration of batteries into PV systems has become imperative to address the intermittent nature of solar energy. Energy storage not only mitigates fluctuations in energy production but also opens avenues for grid-independent power supply. This study explores the symbiotic relationship between Coati-optimized ANFIS MPPT and battery storage, aiming not only to maximize energy capture but also to bolster the stability and quality of the generated power. The research delves into the intricate dynamics of PV-battery-integrated systems, assessing their impact on power quality parameters such as harmonic distortion and voltage stability. By addressing these critical aspects, the proposed optimization strategy contributes to the advancement of sustainable energy solutions, fostering the integration of PV-battery systems into mainstream power grids.

A smart battery controller employing the ANFIS for a PV array integrated into a three-phase grid scheme was introduced in[1)]. The battery charging and discharging process is optimized by the controller based on load demand and solar irradiance. Efficient utilization of the PV system and management of the battery state of charge are ensured by the ANFIS-based controller. In[2)], a Shunt Active Power Filter (SAPF) system powered by a PV battery source designed to enhance power quality and load profiles is presented. The system employs metaheuristic tuning to enhance the control system of the SAPF. This

Cite: N. Pandey, R. Pachauri, "Coati Optimization based ANFIS MPPT for PV-Battery Integrated System to Improve Power Quality". Evergreen, 13 (01) 240-255 (2026). https://doi.org/10.5109/7411064.

proposed system effectively compensates for reactive power, harmonics, and load fluctuations, resulting in improved power quality and load profiles.

Ref[3] presented a Unified Power Quality Conditioner (UPQC) powered by a solar PV battery, controlled by a neural network, for grid-connected operation. Quality of power issues such as sags in grid voltage, swells in grid voltage, and harmonics are effectively alleviated by the UPQC. In[4], an algorithm for peak power extraction based on the current reference regulator is developed, and a power supervision technique for a solar PV battery integrated grid scheme is investigated. The MPPT procedure ensures efficient power extraction from the PV array, while the power management algorithm optimizes battery utilization according to load demand and grid conditions.

Ref[5] demonstrates a coordinated strategy for power supervision and regulation in an isolated PV hybrid scheme. The system incorporates an MPPT algorithm based on modified Invasive Weed Optimization (IWO) to enhance power tracking efficiency. It's significant to note that this study is precise for the combination of an isolated PV hybrid scheme and the adapted MPPT with the IWO algorithm. In[6], a method based on the ANFIS for peak power tracking regulators is developed to maximize power tracking efficiency in a proton exchange membrane fuel cell scheme. The ANFIS-based MPPT controller optimizes the working conditions of the fuel cell system to achieve peak power output under varying loads and environmental conditions.

In[7], an enhanced control method for peak power tracking is introduced using an ANFIS for a proton exchange membrane fuel cell scheme. This method enhances the system's tracking efficiency and stability. A fuzzy logic-based peak power regulator for PV-integrated grid schemes is presented in the research[8], which utilizes a farmland fertility optimization algorithm. The proposed controller optimizes the operating point to enhance the efficiency of power generation in the PV scheme. In[9], a power regulator strategy for a grid-linked inverter in a hybrid renewable energy scheme is developed, employing a Particle Swarm Optimization (PSO) approach. This PSO-based strategy enhances the system's efficiency and stability. It should be acknowledged that this study was conducted in 2015, and advancements in power control strategies may have emerged since then.

In[10], a photovoltaic (PV) scheme with grid-linked battery energy storage is developed, and an adaptive seamless control strategy is optimized using the slime mold algorithm. The system's efficiency and stability are enhanced by the proposed approach. The study in[11] concentrates on the supervision of a hybrid photovoltaic (PV)/battery-isolated scheme under non-uniform irradiance circumstances. A control strategy is proposed to enhance the scheme's performance and alleviate the impact of shading on power generation. In[12], a hybrid regulator for a battery PV-integrated UPQC is presented, utilizing the soccer league optimization algorithm. The proposed controller enhances power quality and system stability. The limitation of this study is its exclusive focus on the soccer league optimization algorithm without comparison with other optimization techniques.

In[13], a modified Marine Predator technique based on obstruction-based knowledge was proposed for trailing the global MPPT of a PV system under uniform irradiance. The primary discovery in this study was that the developed technique outpaced other optimization algorithms in terms of both convergence speed and accuracy. An intelligent regulator approach for a PV/BESS/SOFC integrated grid scheme was introduced in[14]. The key finding of this learning was that the developed regulator approach enhanced the overall system performance and increased the efficiency of energy conversion. A comprehensive study on the role of metaheuristic methods in the application of combined MPPT PV schemes was conducted in[15]. The principal discovery of this study was that metaheuristic algorithms, such as particle swarm optimization and genetic algorithms, effectively optimized the operation of MPPT-PV systems. However, a limitation of this study was the absence of a performance comparison of different metaheuristic algorithms. In[16], an Evolutionary Adaptive Neuro Fuzzy Inference Scheme (EANFIS)-based peak power extraction method was proposed for a standalone PV system. Nevertheless, a limitation of this study was the failure to consider the influence of varying environmental circumstances on the algorithm's performance.

In[17], a novel intelligence and function-based regulator method was introduced for improving the quality of power in a photovoltaic integrated grid scheme. The primary finding of this study was that the proposed technique effectively enhanced power quality and reduced harmonic distortion within the system. The research in[18] investigated the optimum strategy and performance of an artificial neural network (ANN) regulator for a UPQC connected to battery and PV schemes. The main finding was that the ANN controller improved power quality and reduced voltage and current distortions within the system. Nonetheless, a limitation of this study was the omission of consideration for the effects of varying solar irradiance and battery state of charge on controller performance. Investigates using an ANFIS for regulating the frequency in an unsupported microgrid with PV and battery storage. The primary finding of this study was that the ANFIS-based control strategy effectively regulated the microgrid's frequency by adjusting the power output of the PV scheme and battery storage. An intelligent regulator approach for a photovoltaic (PV) integrated grid scheme, a solid oxide fuel cell (SOFC), and a battery energy storage system (BESS) was developed in[20]. The main finding was that the

proposed regulator approach optimized the flow of power between the system components, resulting in improved system performance. However, the study does not provide information about its limitations.

The paper[21] focuses on enhancing the efficiency of a membrane that exchanges protons in a hydrogen fuel cell power system using a fuzzy logic controller. A new bio-enthused metaheuristic procedure for explaining optimization problems, known as the Coati Optimization Algorithm (COA), is presented in this paper[22]. The main finding reveals that, in terms of convergence speed and solution quality, the COA outperforms other metaheuristic algorithms. For wind and PV power prediction in smart grid applications, the paper proposes a hybrid deep learning model called COA-CNN-LSTM[23]. The primary discovery is that the COA-based hybrid model significantly enhances the accuracy of power forecasting when compared to traditional methods. In[24], the paper presents an enhanced COA designed to address the optimal power flow problem, taking into account non-conventional energy uncertainties and electric vehicles. In[25], the updated grey wolf tailored ANFIS resulted in reduced steady state distortions, improved power tracking, and fewer iterations. The DC-DC circuit for PEMFS-interfaced power conversion is designed. This study develops an adaptive PSO-ANFIS controller to extract the highest voltage from the fuel stack[26]. Ref[27] additional metaheuristic optimization-based Maximum Power Point Tracking (MPPT) techniques are investigated in addition to the conventional techniques for figuring out the PEMFS's Maximum Power Point (MPP) position. In[28] discusses the use of hybrid power optimization techniques and a multi-energy storage system using batteries and supercapacitors to integrate renewable energy sources in isolated places. In[29] for PEMFC Fed High Step-Up Single Switch DC-DC Converter uses the grey wolf controller to select fuzzy membership functions. Ref[30] hybrid MPPT techniques optimize both PV and wind turbines. They also present a new power management algorithm that is intended for effective control. To improve the autonomous functioning of a microgrid with multiple DG units, [31] meta-heuristic algorithms are examined for the best design parameters of multiple PI controllers. The coot bird metaheuristic optimizer is used to achieve optimal control of islanded microgrids (MGs) [32], results are validated by comparing them to those obtained using LMSRE-based adaptive control, SFO, Ziegler-Nichols, and PSO approaches. Ref [33] offers an improved technique based on the Lévy Coyote optimization algorithm (LCOA) to solve the Optimal power flow issue with stochastic wind power. In [34], a newly designed circle search method is used to efficiently address the stochastic flow of power. The suggested technique was evaluated on the IEEE 57-bus and 118-bus test systems. Ref[35] describes a probabilistic strategy to controlling the charging load of electric vehicles. A hybrid strategy combines linear programming, dynamic programming, and particle swarm optimization to solve a multi-objective problem in the fuzzy domain.

1.1. Problem Statement & Research Gap

Based on the comprehensive literature survey, it is evident that a variety of intelligent control strategies and optimization algorithms have been proposed for different configurations of renewable energy systems, particularly those integrating photovoltaic (PV) arrays and battery storage. However, a noticeable research gap exists in the lack of a unified and comparative analysis that assesses the applicability and performance of these strategies across diverse PV system architectures and optimization algorithms. Many studies focus on specific configurations, such as three-phase grid-connected PV arrays, PV-battery -SAPF systems, or fuel cell-based systems, limiting the generalizability of their findings. Moreover, there is a dearth of research systematically evaluating the impact of environmental conditions, load variations, and system dynamics on the proposed controllers and optimization algorithms. The literature predominantly lacks a holistic perspective that considers the broader spectrum of PV systems, encompassing both grid-connected and standalone configurations, and addresses the adaptability and robustness of the proposed strategies in dynamic and uncertain operating environments.

Furthermore, the majority of existing studies emphasize the development and evaluation of specific optimization algorithms without comprehensive comparisons among different metaheuristic techniques. This limitation hinders the identification of the most suitable algorithm for specific applications and system architectures. A critical research gap is evident in the absence of studies that systematically compare the performance of various metaheuristic algorithms, such as Genetic Algorithm, PSO, and Marine Predator Algorithm, in the context of optimizing PV systems. Bridging these gaps is essential for advancing the understanding of intelligent control strategies and optimization algorithms in the broader context of renewable energy systems and the implementation of these technologies for diverse PV configurations and environmental conditions. In this paper, Coati Optimization-based ANFIS MPPT for PV-Battery Integrated System to Improve Power Quality is presented to mitigate the above problem. The organization of the paper is shown in Figure1.

2. Grid Connected PV- Battery system Modeling

The PV battery liked grid scheme is shown in, and it includes a ripple filter, a voltage source converter, interface inductors, a PV grid with a three-phase scheme, battery energy storage, nonlinear loads, and unbalanced

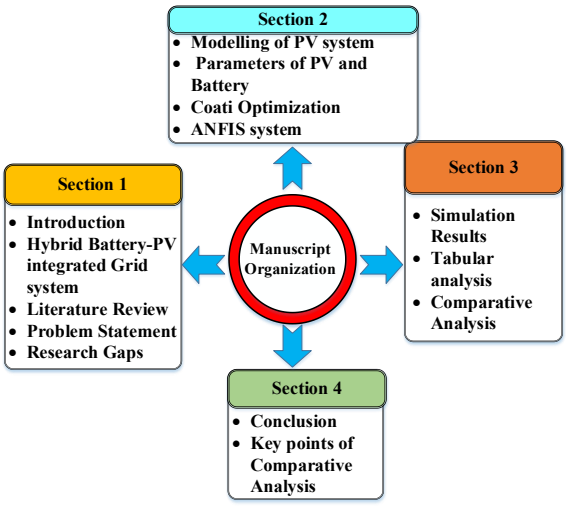

Fig. 1: Manuscript Organization

loads. Harmonics at higher order are formed by the voltage source inverter switching ripple and are condensed by the ripple filter. An interface inductor is used to reduce current harmonics in PV battery-linked voltage source converters. A battery is linked to a DC bus link through a DC-DC bidirectional converter.

The array of PV panels is operated using the Coati-ANFIS-based peak power extractor algorithm to maximize power production. The current control method is employed to excerpt the quadrature component of the vital current of the load. The regulator procedure comprises Coati-ANFIS techniques and control of the switching of the voltage source converter. The Coati-ANFIS techniques are used to produce the reference DC link voltage as depicted in Figure.2.

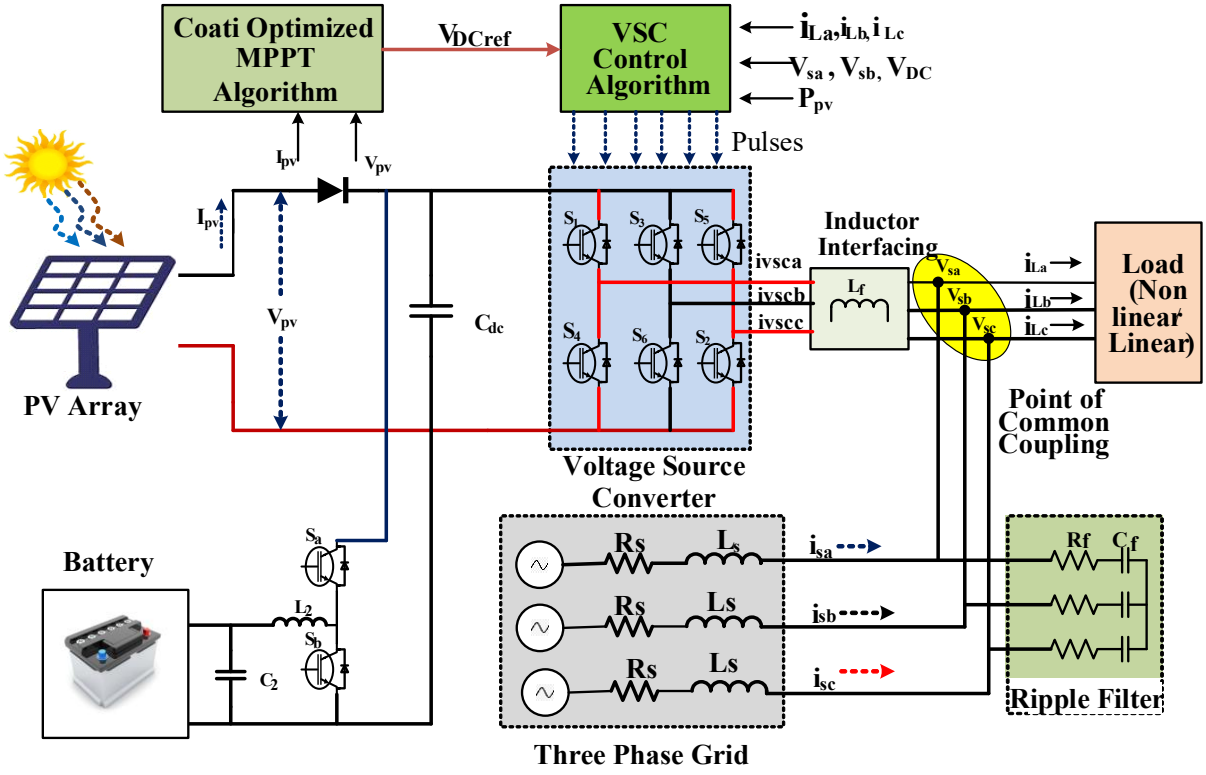

Fig. 2: PV Battery Grid Connected System with Coati optimization based MPPT control

Table 1: PV Parameter & Specification

Parameters	Values
Voltage of Open Circuit	36.3 V
Current of Short Circuit	7.84 A
Cells per module	60
Number of Series linked units per string	25
Number of Parallel linked modules per string	18
Maximum power voltage (V_{mp})	29 V
Maximum power current (I_{mp})	7.35 A
Resistance at shunt R_{sh}	313.05 Ω
Resistance at series R_s	0.39 Ω

Table 1 provides crucial parameters related to a photovoltaic module, offering insights into its electrical characteristics and configuration. Table 2 presents essential parameters related to a lithium-ion battery, providing valuable information about its characteristics and performance.

Table 2: Battery Specifications

Parameters	Values
Voltage at rated operation	480 V
Capacity at rated operation	500 Ah
State of Charge at Initial	50 %
Response Time of Battery	Sec

Cite: N. Pandey, R. Pachauri, "Coati Optimization based ANFIS MPPT for PV-Battery Integrated System to Improve Power Quality". Evergreen, 13 (01) 240-255 (2026). https://doi.org/10.5109/7411064.

2.1. Coati optimization technique

The coatis engage in sophisticated behavior while pursuing and evading predators, as well as when attacking and killing iguanas. The basic source of design inspiration for the suggested COA technique was the imitation of these coati's ordinary activities. The developed COA is described in this section, and its many phases are mathematically modeled.

2.1.1. Algorithm initialization process

Coatis are regarded as members of the population within the COA method, which is a metaheuristic approach based on populations. Coati placements in the search space modify selection factor values. Thus, the coatis' perspective may solve the COA method's problem. Eq. (1) randomizes coatis' search space positions at the start of COA implementation.

$$X_i: x_{i,j} = lb_j + r.\left(ub_j - lb_j\right), i = 1,2,\dots,N, j = 1,2,\dots,m, \quad (1)$$

In the given equation (1), Xi represents the positioning of the ith coati within the search space, while xi,j denotes the value assigned to the jth decision variable. N signifies the total count of coatis, m stands for the count of decision variables, r signifies a randomly generated real number falling within the [0, 1] range, and l_{bj} and u_{bj} correspond to the lower and upper bounds of the j^{th} decision variable, respectively. The population matrix, which can also be referred to as the matrix denoted by X, serves as a mathematical depiction of the coati population within the COA method:

$$X = \begin{bmatrix} X_1 \\ \vdots \\ X_i \\ \vdots \\ X_N \end{bmatrix}_{N\times m} = \begin{bmatrix} x_{1,1} & \cdots & x_{1,j} & \cdots & x_{1,m} \\ \vdots & \ddots & \vdots & \ddots & \vdots \\ x_{i,1} & \cdots & x_{i,j} & \cdots & x_{i,m} \\ \vdots & \ddots & \vdots & \ddots & \vdots \\ x_{N,1} & \cdots & x_{N,j} & \cdots & x_{N,m} \end{bmatrix}_{N\times m} \quad (2)$$

The arrangement of potential solutions within decision variables leads to the evaluation of diverse values for the problem's objective function. These values are demonstrated using Eq. (3).

$$F = \begin{bmatrix} F_1 \\ \vdots \\ F_i \\ \vdots \\ F_N \end{bmatrix}_{N\times 1} = \begin{bmatrix} F(X_1) \\ \vdots \\ F(X_i) \\ \vdots \\ F(X_N) \end{bmatrix}_{N\times 1} \quad (3)$$

The consequent objective function from the i^{th} coati is Fi, where F is the vector of objective function values. In metaheuristic algorithms, such as the one introduced in the COA method, the objective function's value acts as the yardstick for evaluating the quality of potential solutions. The population member that leads to the determination of the most optimal objective function value is designated as the finest population member. With the continuous updating of candidate solutions throughout each iteration of the algorithm, the best population member undergoes corresponding updates.

2.2. Scientific model of COA

Modeling coatis' two inherent tendencies underpins altering coati's locations (possible solutions) in the COA. These actions include:

The strategies employed by coatis in their attacks on iguanas and

The ways in which they flee from predators.

As a result, there are two distinct periods for updating the COA population.

2.2.1. Phase 1: Stalking and assaultive approach on iguana (exploration phase)

The initial iteration of updating the coati population within the search region is emulated through a simulation of their tactics for engaging iguanas. In this procedure, a multitude of coatis ascend trees to approach an iguana, initiating a startle response. Meanwhile, additional coatis congregate beneath the tree, anticipating the iguana's descent to the ground. Once the iguana lands, the coatis launch an attack and pursue it. By employing this approach, coatis demonstrate their ability to relocate across various positions within the search region, thereby highlighting the COA's effectiveness in conducting a comprehensive search within the problem-solving domain. The COA assumes the iguana is the population's best member. It also suggests that half the coatis ascend the tree and half wait for the iguana to fall. Eq. (4) captures coatis' positions after emerging from the tree.

$$X_i^{P1}: x_{i,j}^{P1} = x_{i,j} + r(Iguana_i - I.x_{i,j}) \quad (4)$$

The iguana descends and is randomly relocated in the search area. Based on this randomly selected location, ground-based coatis navigate the search space using Eqs. (5) and (6).

$$Iguana^G: Iguana_j^G = lb_j + r.\left(ub_j - lb_j\right), \quad j = 1,2,\dots,m, \quad (5)$$

$$X_i^{P1}: x_i^{P1} = \begin{cases} x_{i,j} + r\left(Iguana_j^G - Ix_{i,j}\right), F_{Iguana}G < F_i \\ x_{i,j} + r(x_{i,j} + r\left(x_{i,j} - Iguana_j{}^G\right), else \end{cases}$$

$$for\ i = [N/2] + 1, [N/2] + 2, \dots, N\ and\ j = 1,2,\dots,m \quad (6)$$

In the event that the modified position of any coati results in an enhancement of the objective function's value, such

a change is considered permissible within the updating procedure. Conversely, if the altered position fails to yield an improvement, the coati retains its prior location. This criterion for updates is consistently reproduced through Eq. (7), applicable for i = 1, 2…, N.

$$X_i = \begin{cases} X_i^{P1}, F_i^{P1} < F_{i,} \\ X_i, else \end{cases} \quad (7)$$

Meanwhile, Iguana G pertains to the ground-based location of the iguana, established through random generation. XP1 i signifies the fresh position computed for the ith coati. The schematic illustration of the initial stage of COA is presented in, encapsulating its pattern diagram. Figure 3 (a) showcases the engagement of fifty percent of the coati population in an attack directed towards the iguana located on the tree, Fig 3. (b) Portrays the pursuit of the fallen iguana on the ground by the remaining fifty percent of the coati population.

(a)

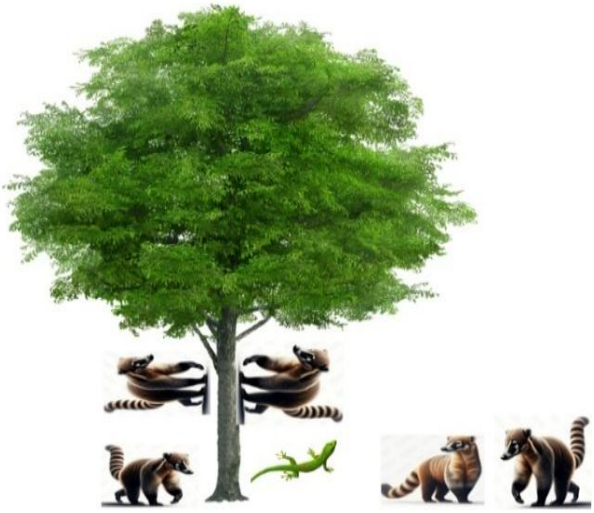

(b)

Fig. 3: The schematic representation of the initial phase within the COA

2.2.2. Phase 2: The course of absconding from hunters (exploitation phase)

The mathematical representation of the second phase, involving the adjustment of coatis' positions within the search space, is established based on their customary behaviors when confronted with and evading predators. Utilizing Eqs. (8) and (9), a random position is generated in proximity to the location of each coati to simulate this specific behavior.

$$lb_j^{local} = \frac{lb_j}{t}, ub_j^{local} = \frac{ub_j}{t}, where\ t = 1, 2, \ldots, T \quad (8)$$

$$X_i^{P2}: x_{i,j}^{P2} = x_{i,j} + (1 - 2r).\left(lb_j^{local} + r.\left(ub_j^{local} - lb_j^{local}\right)\right),$$

$$i = 1, 2, \ldots, N, j = 1, 2, \ldots, m, \quad (9)$$

Should the newly derived location lead to an enhancement in the objective function's value, this condition, as stipulated by Eq. (10), is deemed met and, thus, acceptable.

$$X_i = \begin{cases} X_i^{P2}, F_i^{P2} < F_i, \\ X_i, else \end{cases} \quad (10)$$

In this context, Fi^{P2} represents the objective function's value, and X_i^{P2} corresponds to the newly computed position for the i^{th} coati, which stems from the second phase of COA. Additionally, $x_{i,\ j}^{P2}$ pertains to the j^{th} dimension of this position, while r denotes a randomly generated number within the range [0, 1]. Furthermore, t signifies the iteration counter, and lb_{jlocal} and ub_{jlocal} respectively stand for the local lower bound and local upper bound of the j^{th} decision variable.

2.3. Adaptive Neuro Fuzzy Inference System

The ANFIS architecture, comprising five layers, is depicted in Figure 4. Unlike scatter division, tiered partition, and fuzzy c-mean techniques, the grid partition method reduces the rule count to a manageable level by dividing the input space into subsets that are expected to encompass input vectors. Layer 1, often denoted as the input layer, is where the input is subjected to fuzzification. In this layer, the fuzzy system assigns membership values to each input space subset using an algebraic equation, as defined by the formula.

$$o_{ij}^{(1)} = \mu_j(I_{ij}^{(1)}) \quad (11)$$

Layer 2, referred to as the Fuzzy-AND operation layer within the ANFIS architecture, represents the second stage. In this layer, each node executes a FUZZY-AND operation, employing the algebraic product's T-norm operator. The output of each node is determined by calculating the

product of its respective outcome.

$$o_k^{(2)} = \omega_k = \prod_{i=1}^{q} o_{ij}^{(1)} \quad (12)$$

The normalizing layer is the third level of the ANFIS architecture. Its objective is to calculate each node's output by dividing the activation value of each code in the fuzzy system by the total number of activation values. The initiation standards of the fuzzy rules are normalized in this stage to make sure that each one contributes fairly to the outcome.

$$o_k^{(3)} = \overline{\omega_k} = \frac{o_k^{(2)}}{\sum_{m=1}^{y^2} o_m^{(2)}} \quad (13)$$

In the ANFIS architecture, the fourth layer is comprised of nodes featuring linear parameters. Each node, denoted as "k", applies a straightforward function represented by an equation and possesses an associated set of adjustable parameters (d1k, d2k, ..., dyk, d0).

$$o_k^{(4)} = \overline{\omega_k} f_k = \overline{\omega_k} (d_{1k} I_1^{(1)} + d_{2k} I_2^{(1)} + \cdots + d_{yk} I_y^{(1)} + d_0) \quad (14)$$

The fifth layer of the ANFIS model features a single node responsible for algebraically summing up all the inputs to generate the network's output. The optimization of ANFIS parameters is achieved through the utilization of the Coati Optimization technique, which is elaborated on in the subsequent section.

2.3.1. Coati-ANFIS Control for Maximum Power Extraction

The Coati-ANFIS technique is used to regulate the peak power point. Based on the input and target data provided to the ANFIS scheme, the Coati algorithm is utilized to

$$U_a = o^5 = \sum_{k=1}^{y^2} o_k^{(4)} = \sum_{k=1}^{y^2} \overline{\omega_k} f_k = \frac{\sum_{k=1}^{y^2} \omega_k f_k}{\sum_{k=1}^{y^2} \omega_k} \quad (15)$$

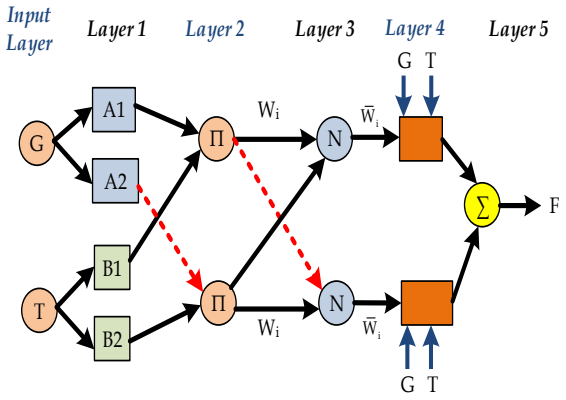

Fig. 4: Layers of ANFIS Network

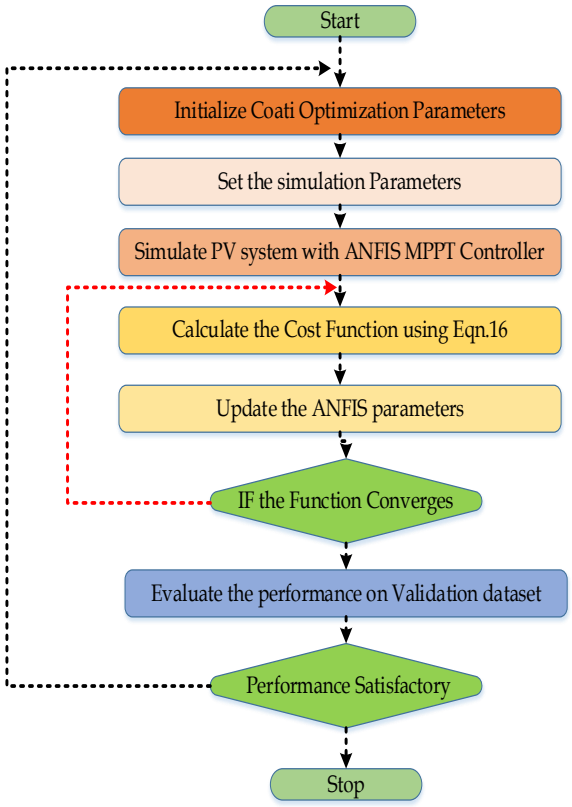

Fig. 5: Flowchart of Coati based ANFIS MPPT Controller

tune the ANFIS parameter. The ANFIS system receives input information about the PV's irradiance and temperature and output information about the PV's voltage under maximum power point circumstances. The Coati techniques are utilized to fine-tune the ANFIS input and output membership function values and rules between input and output. The ANFIS Network is used to maximize the energy from solar panels and provide position voltage for the DC bus voltage regulator after training with the Coati algorithm. Figure 4 illustrates the five-layer ANFIS network, while Figure 5 displays the flowchart for Coati Optimized ANFIS MPPT and training.

The Coati technique fine-tunes the parameters of the ANFIS model according to the following objective function:

$$objective\ function = \sqrt{(V_{ref} - V_{act})^2} \quad (16)$$

Where, V_{ref} is the target reference voltage and V_{act} is the actual voltage from the ANFIS system.

3. Simulation Results

A simulation has been developed for Coati Optimization-based ANFIS MPPT in a PV battery-integrated system with the aim of enhancing power extraction and power quality. This simulation was meticulously crafted and rigorously tested using MATLAB 2020a. The input and

target voltages are shown in Figure 6 (a to c), and the convergence graph of the Coati algorithm for ANFIS tuning is shown in Figure 6 (d). The training error and testing error details are shown in Figure 7(b). The training error is around 1.4842E-13, and the testing error is around 1.4895E-13.

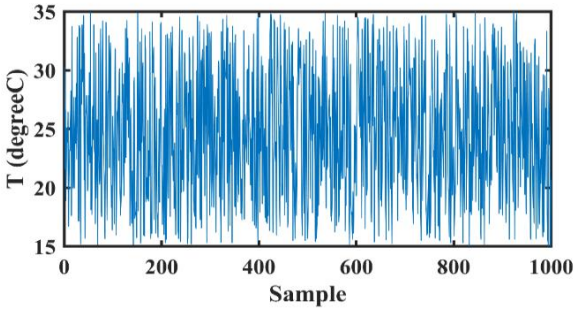

(a)

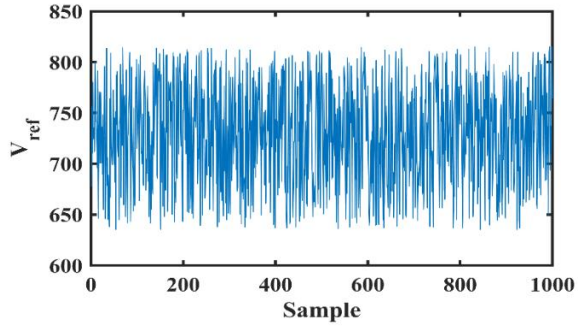

(b)

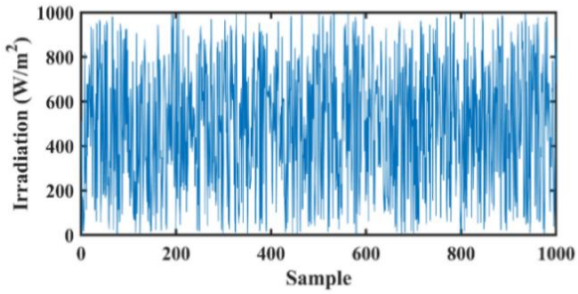

(c)

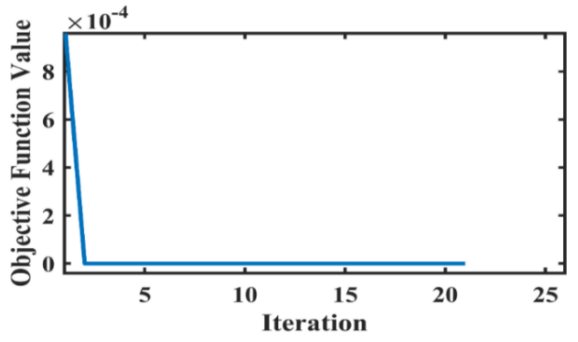

(d)

Fig. 6: (a) Irradiance data, b) Target voltage, c) Temperature data and d) Convergence graph by Coati

Figure 8 shows the rule of the ANFIS-trained Coati optimization. The Coati Optimization-based ANFIS MPPT was subjected to PV battery grid tests under various operational conditions, including scenarios of constant irradiance, fluctuating irradiance, and changing temperature conditions.

To assess its performance and efficiency, the proposed

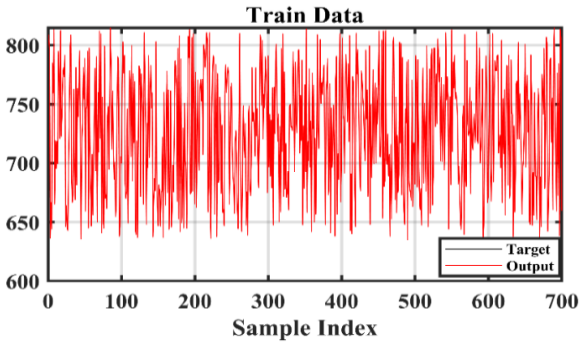

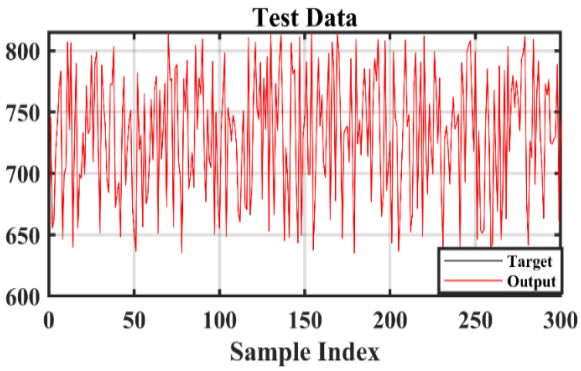

(a)

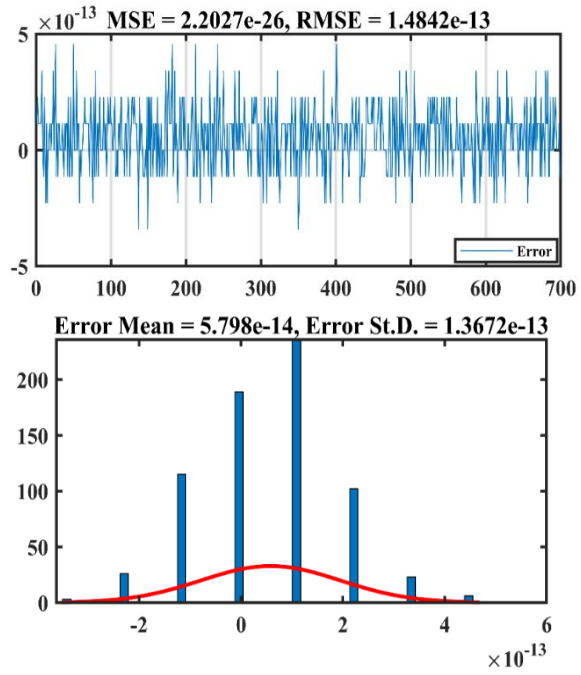

(b)

Fig. 7: (a) Training Error details and (b) Testing Error details

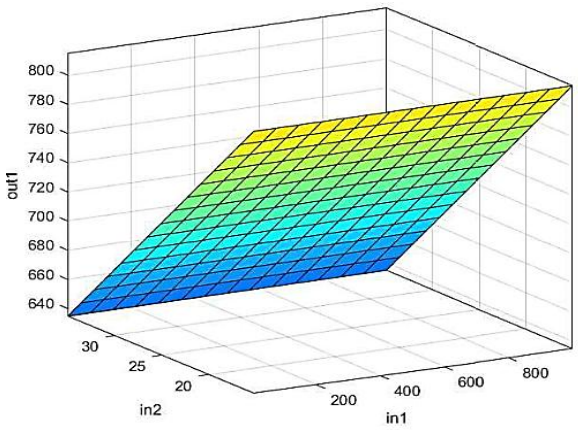

Fig. 8: Rule for input and output

Coati-optimized ANFIS MPPT technique was benchmarked against several existing MPPT methods, including PSO-ANFIS, GWO-ANFIS, and FP-ANFIS. This comparative analysis was conducted to gauge the superiority and potential advantages of the Coati optimization-based approach in the realm of PV-battery grid systems.

3.1. Case: 1 Constant Irradiance

The system is tested with constant irradiance, i.e., the irradiance of the PV panel is fixed at 1000 W/m2 and the temperature is fixed at 25 ºC. The PV voltage and current power are shown in Figure 9. The performance parameters such as voltage, current, power, settling time, rise time, and efficiency are depicted in Table 3.

Table 3 provides a detailed comparison of different MPPT methods, specifically examining their performance based on various parameters. MPPT techniques are crucial in optimizing power generation in photovoltaic systems by ensuring that solar panels operate at their maximum power output, even under varying environmental conditions. Each row in the table represents a different MPPT technique, including PSO, GWO, FP (Flower Pollination Optimization), and Coati. The "Voltage (V)" and "Current (A)" columns indicate the voltage and current values at which these techniques operate. These values play a vital role in determining the electrical output of the photovoltaic system. "Power (KW)" shows the power output in kilowatts achieved by each technique, with Coati delivering the highest power of 95.8 kW, closely followed by PSO with 93.9 kW. The "Rise Time (s)" and "Settling Time (s)" columns provide insights into how quickly each

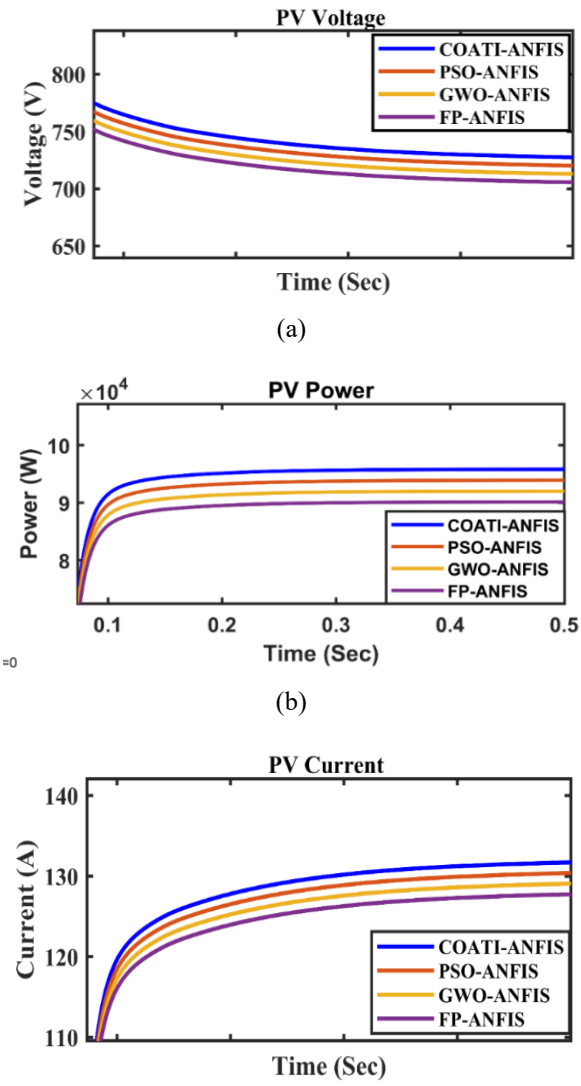

Fig. 9: (a) PV Voltage (b) PV Current & (c) PV Power during constant irradiance conditions

technique responds to changes in environmental conditions and how long it takes for the system to stabilize at its new operating point. The smaller values in these columns suggest that the MPPT technique can adapt rapidly to changes, which is advantageous in real-world scenarios where weather conditions may fluctuate. Lastly, the "Efficiency " column evaluates the overall efficiency of each MPPT technique. Coati stands out with an impressive efficiency of 99.3%, indicating its ability to maximize power generation while minimizing energy losses.

Table 3: Performance Evaluation of the MPPT Techniques at constant irradiance

MPPT Technique	Voltage (V)	Current (A)	Power (KW)	Rise time (Sec)	Settling time (Sec)	Efficiency (%)
PSO	720.2	130.4	93.9	0.06	0.16	98.6
GWO	712.9	129.1	92.02	0.09	0.2	96.4
FP	705.7	127.8	90.15	0.08	0.19	97.2
Coati	727.5	131.7	95.8	0.06	0.11	99.3

Cite: N. Pandey, R. Pachauri, "Coati Optimization based ANFIS MPPT for PV-Battery Integrated System to Improve Power Quality". Evergreen, 13 (01) 240-255 (2026). https://doi.org/10.5109/7411064.

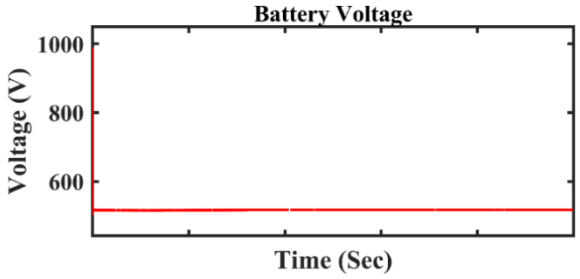

(a)

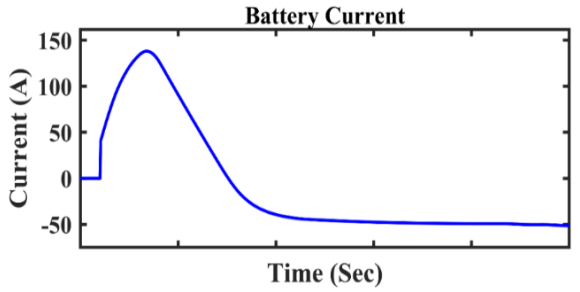

(b)

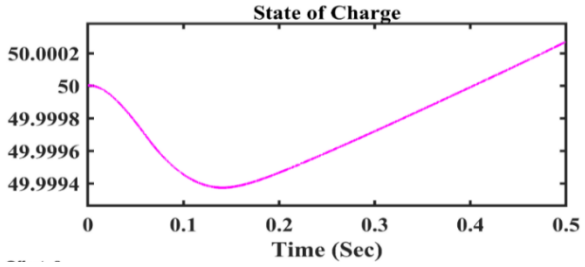

(c)

Fig. 10: (a) Battery Voltage (b) Battery Current & (c) SOC of Battery during constant irradiance conditions

Figure 10 illustrates key data related to the battery, including its voltage, current, and state of charge. The battery voltage remains constant at 517.6 volts, with the battery current initially peaking at 140 A and subsequently decreasing to -50 A within 0.15 seconds. Notably, the battery remains in a continuous charging state throughout these conditions. Moving on to Figure 11, we present data pertaining to the inverter, showcasing its voltage and current characteristics. The inverter voltage is consistently maintained at a peak of 325 volts, while the inverter current remains stable at 126 A at its peak.

Figure 12 provides insight into the load, displaying voltage and current parameters. The load voltage maintains a peak of 325 volts, and the load current holds steady at 20 A at its peak. The THD of the current, which is maintained at a low value of 27.99%, is shown in Figure 13.

In Figure 14, we shift our focus to the grid, where we observe grid voltage and current details. The grid voltage maintains a peak of 325 volts, while the grid current is consistently held at 125 A at its peak. Furthermore, Figure

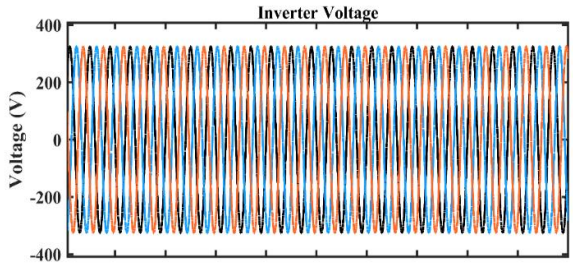

(a)

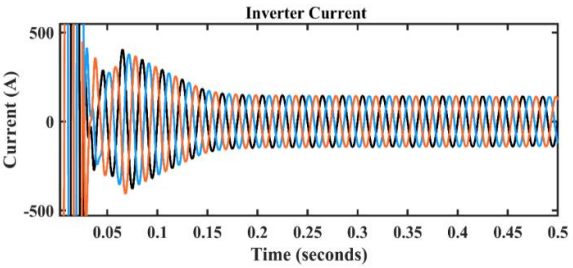

(b)

Fig. 11: Voltage & Current of Inverter during constant irradiance conditions

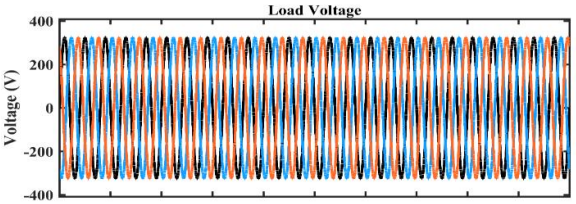

(a)

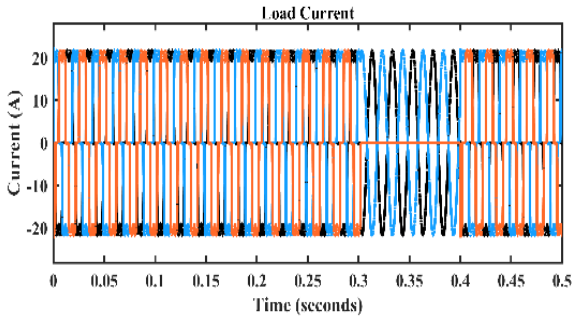

(b)

Fig. 12: (a) Load Voltage (b) Load Current during constant irradiance conditions

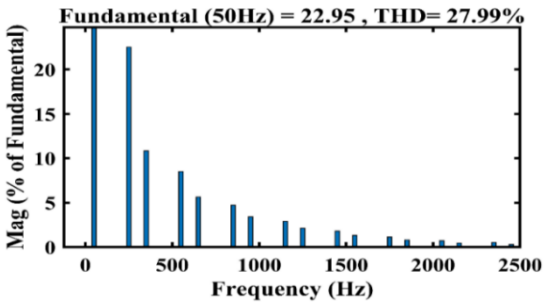

Fig. 13: THD of the Load current during constant irradiance conditions

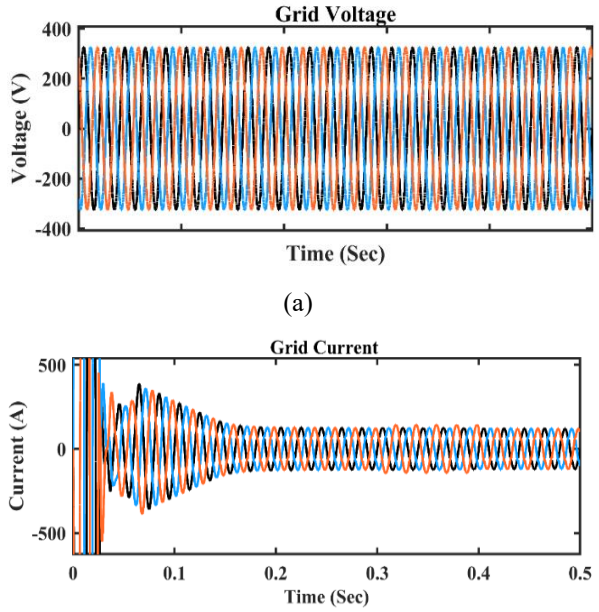

Fig. 14: (a) Grid Voltage (b) Grid Current during constant irradiance conditions

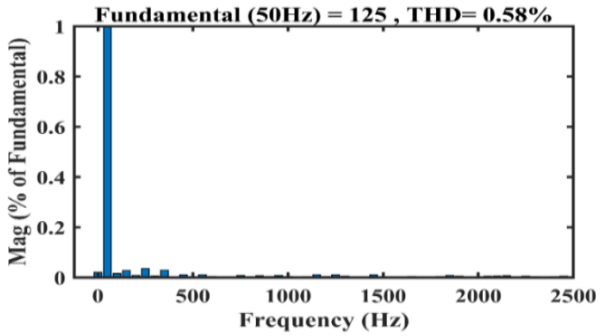

Fig. 15: THD of the grid current during constant irradiance conditions

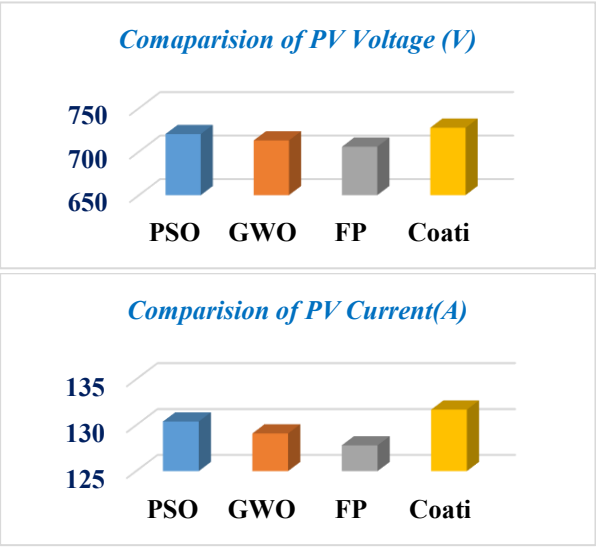

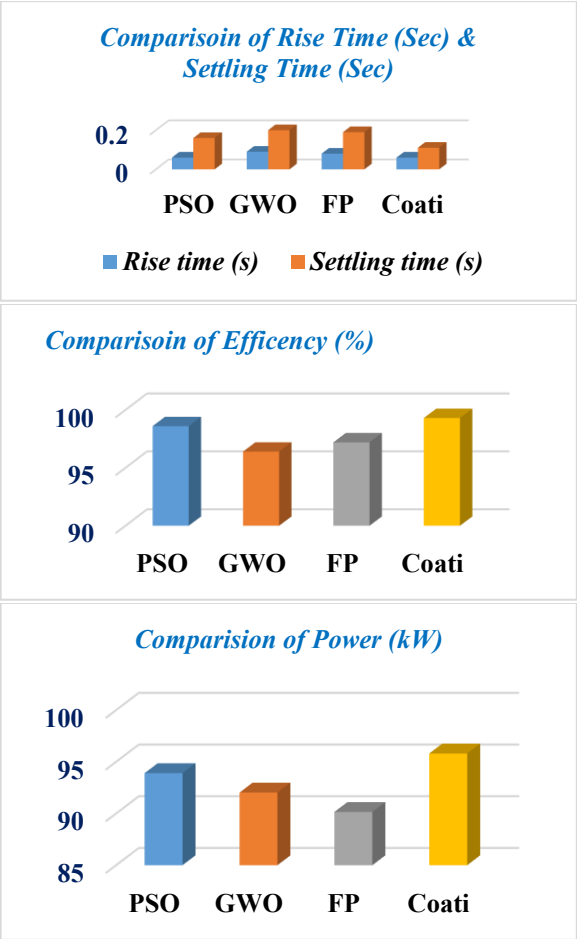

Fig. 16: Comparative Analysis of Table 3

15 presents the THD of the current, which is maintained at a low value of 0.58%. It is worth noting that this THD value adheres to the standards set forth in EEE 519-2022, ensuring compliance with established quality and safety guidelines. Figure 16 represents the comparative analysis for case-1.

3.2. Case 2: Varying Irradiance

The system test has varying irradiance conditions, i.e., the irradiance of the PV panel is fixed at 700 W/m2 between 0.3 and 0.6 seconds, 500 W/m2 between 0.6 and 0.9 seconds, and 400 W/m2 between 0.9 and 1.2 seconds (the temperature is fixed at 25ºC in a). The PV voltage and current power are shown in Figure 17. The performance parameters, such as voltage, current, power, settling time, rise time, and efficiency, are depicted in Table 4.

Table 4 provides a comprehensive performance evaluation of various MPPT techniques under different irradiance levels. Coati consistently demonstrates its superiority over the other MPPT techniques in the provided table, showcasing exceptional performance across varying irradiance levels. At an irradiance of 700 W/m², Coati achieves a remarkable PV power output of 67.06 KW with a mere 0.31 second rise time and 0.35-

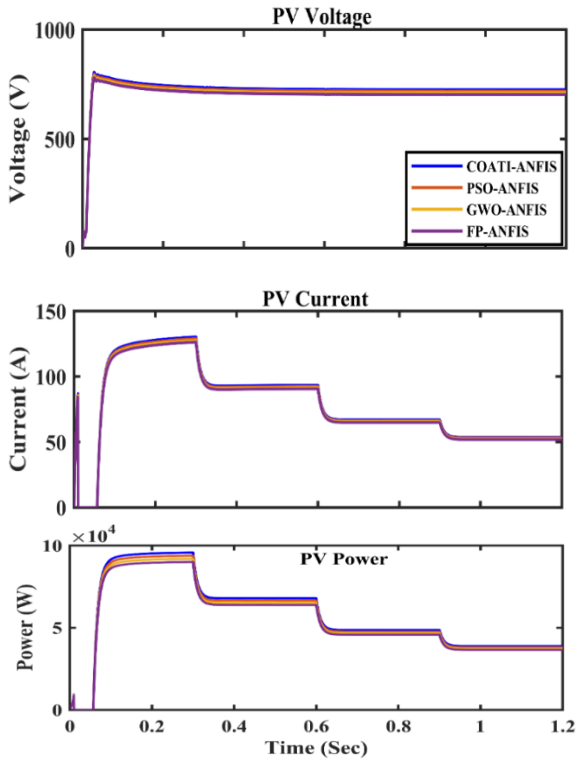

Fig. 17: Voltage Current & Power of PV Array during varying irradiance conditions

second settling time, resulting in an impressive efficiency of 98.307%. These metrics reflect Coati's capability to maximize power generation and swiftly respond to fluctuating irradiance. Furthermore, even at lower irradiance levels (500 W/m² and 400 W/m²), Coati maintains its lead with the highest PV power output and efficiency, emphasizing its robust performance.

On the other hand, competitive MPPT techniques such as PSO, GWO, and FP consistently lag behind Coati's performance. Under an irradiance level of 700 W/m², PSO achieves a PV power output of 65.73 KW, featuring a rise time of 0.38 seconds, a settling time of 0.45 seconds, and an efficiency of 97.614%. Similarly, GWO generates 64.414 KW with a rise time of 0.35 seconds, a settling time of 0.42 seconds, and an efficiency of 95.436%, while FP reaches 63.105 KW with a rise time of 0.32 seconds, a settling time of 0.4 seconds, and an efficiency of 96.228%. Although these values demonstrate competitiveness, PSO, GWO, and FP consistently find themselves outperformed by Coati. Coati excels as the most efficient and responsive MPPT technique, ensuring optimal power generation and rapid adaptation to changing sunlight conditions.

Table 5 provides data in compliance with the IEEE 519-2022 standard, indicating the THD of the grid current at different irradiance conditions (700 W/m², 500 W/m², and 400 W/m²). THD represents the extent of harmonic distortion in the grid current, which is a critical parameter to ensure the quality of electrical power in grid-connected systems. Under an irradiance of 700 W/m², the THD of the grid current is 1.3%, indicating low harmonic

Table 4: Performance Evaluation of the MPPT techniques at varying irradiance

Method	Irradiance: 700 W/m²			
	Power (KW)	Rise time (s)	Settling time (s)	Efficiency (%)
PSO	65.73	0.38	0.45	97.614
GWO	64.414	0.35	0.42	95.436
FP	63.105	0.32	0.4	96.228
Coati	67.06	0.31	0.35	98.307
Method	Irradiance: 500 W/m²			
	Power (KW)	Rise time (s)	Settling time (s)	Efficiency (%)
PSO	46.95	0.68	0.72	96.628
GWO	46.01	0.68	0.71	94.472
FP	45.075	0.65	0.68	95.256
Coati	47.9	0.63	0.65	97.314
Method	Irradiance: 400 W/m²			
	Power (KW)	Rise time (s)	Settling time (s)	Efficiency (%)
PSO	37.56	0.98	1.03	96.135
GWO	36.808	0.96	1.01	93.99
FP	36.06	0.94	0.97	94.77
Coati	38.32	0.92	0.94	96.8175

Table 5: THD of the grid current at varying irradiance with Coati

Condition	Irradiance: 700 W/m²	Irradiance: 500 W/m²	Irradiance: 400 W/m²
THD of the grid Current (%)	1.3	2.5	4.3

distortion and good power quality. At 500 W/m² irradiance, the THD increases to 2.5%, suggesting a slightly higher level of harmonic distortion. However, at 400 W/m², the THD further increases to 4.3%, signifying a notable increase in harmonic distortion. These values adhere to the IEEE 519-2022 standard, which sets guidelines for the permissible levels of harmonic distortion to maintain the quality of power in grid-connected systems.

3.3. Case 3: Varying Temperature

The system test with varying temperature conditions, i.e., the temperature of the PV panel, is fixed at 20ºC between 0.3 and 0.6 seconds, 15 ºC between 0.6 to 0.9 seconds, and 10ºC between 0.9and 1.2 seconds (temperature is fixed at 25 ºC in a). The PV voltage and current power are shown

in Figure 18. The performance parameters, such as power, settling time, rise time, and efficiency are depicted in Table 6.

Table 6 presents a comprehensive performance evaluation of various MPPT techniques under different temperature conditions, specifically at 20ºC, 15ºC, and 10ºC. Once again, the "Coati" MPPT technique consistently stands out as the top performer. At 20ºC, Coati achieves the highest PV power output at 96.758 KW, with a swift rise time of 0.31 seconds and a settling time of 0.33 seconds, resulting in an impressive efficiency of 99.0021%. These figures demonstrate Coati's exceptional ability to maximize power generation and its efficiency in tracking the maximum power point, even under varying temperature conditions.

In contrast, the other MPPT techniques, namely PSO, GWO, and FP, exhibit competitive performance but consistently fall behind Coati. At a temperature of 20ºC, PSO yields a PV power output of 94.839 KW, accompanied by a rise time of 0.38 seconds, a settling time of 0.43 seconds, and an efficiency of 98.3042%. Similarly, GWO generates 92.9402 KW with a rise time of 0.35 seconds, a settling time of 0.42 seconds, and an efficiency of 96.1108%. Meanwhile, FP achieves 91.0515 KW with a rise time of 0.32 seconds, a settling time of 0.41 seconds, and an efficiency of 96.9084%. However, all these methods consistently trail Coati's performance in the given conditions. This pattern of Coati's superior

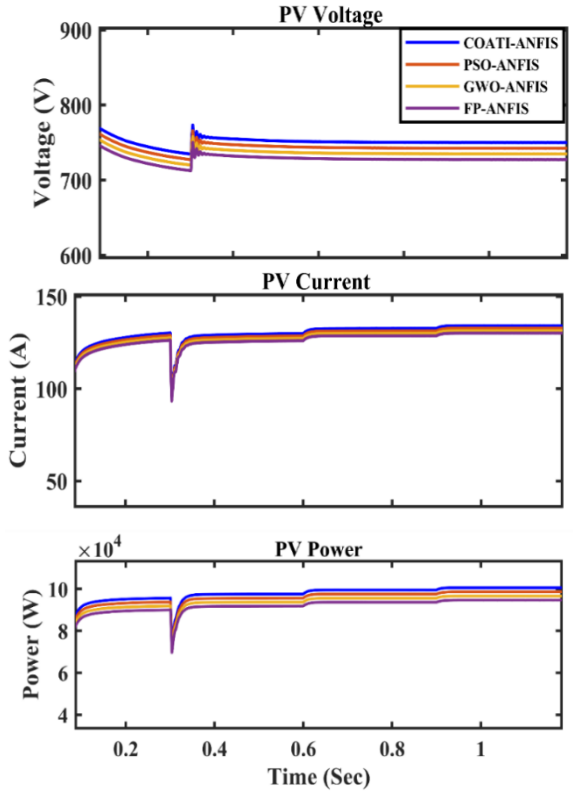

Fig. 18: Voltage Current & Power of PV Array during Constant irradiance & varying temperature conditions

Table 6: Performance Evaluation of the MPPT Techniques at varying temperature

Method	Temperature: 20ºC			
	Power (KW)	Rise time (s)	Settling time (s)	Efficiency (%)
PSO	94.839	0.38	0.43	98.3042
GWO	92.9402	0.35	0.42	96.1108
FP	91.0515	0.32	0.41	96.9084
Coati	96.758	0.31	0.33	99.0021
Method	Temperature: 15ºC			
	Power (KW)	Rise time (s)	Settling time (s)	Efficiency (%)
PSO	96.717	0.69	0.72	97.121
GWO	94.7806	0.67	0.71	94.954
FP	92.8545	0.65	0.68	95.742
Coati	98.674	0.62	0.65	97.8105
Method	Temperature: 10ºC			
	Power (KW)	Rise time (s)	Settling time (s)	Efficiency (%)
PSO	98.595	0.98	1.02	96.1843
GWO	96.621	0.95	1	94.0382
FP	94.6575	0.94	0.97	94.8186
Coati	100.59	0.93	0.94	96.8672

Table 7: THD of the grid current at varying temperatures with Coati

Temperature:	20ºC	15ºC	10ºC
THD of the grid Current (%)	0.61	0.63	0.68

performance is consistent at lower temperatures. At 15ºC, Coati maintains the highest PV power output, efficiency, and response times. At 10ºC, Coati once again leads with a PV power output of 100.59 KW, an efficiency of 96.8672%, and competitive response times.

In summary, Coati consistently proves to be the most efficient and responsive MPPT technique, delivering the highest PV power output and efficiency under varying temperature conditions.

The provided Table 7 conforms to the IEEE 519-2022 standard, which governs the quality of electrical power in grid-connected systems by presenting data on the THD of the grid current under different temperature conditions. It reports the THD of the grid current at temperatures of 20ºC, 15ºC, and 10ºC. The values, 0.61%, 0.63%, and 0.68%, demonstrate the level of harmonic distortion in the grid current at each temperature. These figures indicate a low level of harmonic distortion, which aligns with the IEEE 519-2022 standard's requirements for maintaining

the quality of power in grid-connected systems. Low THD values signify that the electrical power system is operating within acceptable limits, ensuring that the grid current remains relatively free from harmonics, thereby meeting the specified standards for power quality.

4. Conclusion

In conclusion, this research introduces a groundbreaking approach that significantly enhances the performance of photovoltaic (PV) systems when integrated with batteries, with a primary focus on MPPT and the improvement of power quality. The study creates a precise and effective MPPT process that easily adjusts to changing solar conditions by combining the new Coati optimization algorithm with the ANFIS. The Coati algorithm optimizes the tracking procedure to ensure optimal energy harvest from PV modules. It takes inspiration from the cooperative foraging behaviour of coatis. Moreover, the incorporation of battery storage into the system effectively addresses the intermittency challenges associated with solar energy production, providing reliability and stability to the power output. In particular, this study looks at the bigger picture by looking at how optimization affects power quality parameters like voltage stability and harmonic distortion. This is important for ensuring smooth grid integration and compatibility with different loads. The simulation validation underscores the superiority of this proposed approach when compared to traditional MPPT techniques. The key findings of the research are illustrated below:

Constant Irradiance: The system achieved 99.3% efficiency, surpassing PSO (98.2%) and GWO (96.4%), while maintaining a low THD of 0.58%, well within permissible limits.

Varying Irradiance: At irradiance levels of 700 W/m², 500 W/m², and 400 W/m², grid current THD values were 1.3%, 2.5%, and 4.3%, respectively—all below the IEEE 519-2022 standard.

Varying Temperature: Grid current THD remained stable across temperature variations, recorded at 0.61% (20°C), 0.63% (15°C), and 0.68% (10°C).

This research emphasizes the critical importance of implementing advanced optimization strategies within PV-battery-integrated systems. These strategies not only maximize energy capture but also ensure the delivery of high-quality power supplies. Consequently, this study makes a significant contribution to advancing sustainable energy systems by offering an innovative solution that enhances the efficiency and reliability of PV-battery-integrated systems. Such advancements promote the widespread adoption of these systems in modern power grids, marking a pivotal step towards a more sustainable and dependable energy future.

References

1) M. M. Ismail and A. F. Bendary, Smart battery controller using ANFIS for three phase grid connected PV array system, Mathematics and Computers in Simulation, vol. 167, pp. 104–118, 2020. DOI: 10.1016/j.matcom.2018.04.008
2) R. Kumar, H. O. Bansal, and D. Kumar, Improving power quality and load profile using PV-battery-SAPF system with metaheuristic tuning and its HIL validation, International Transactions on Electrical Energy Systems, vol. 30, no. 5, pp. e12335, 2020. DOI: 10.1002/2050-7038.12335
3) O. E. Okwako et al., Neural network controlled solar PV battery powered unified power quality conditioner for grid connected operation, Energies, vol. 15, no. 18, pp. 6825, 2022. DOI: 10.3390/en15186825
4) P. K. Sorte, K. P. Panda, and G. Panda, Current reference control based MPPT and investigation of power management algorithm for grid-tied solar PV-battery system, IEEE Systems Journal, vol. 16, no. 1, pp. 386–396, 2021. DOI: 10.1109/JSYST.2021.3052959
5) C. Pradhan et al., Coordinated power management and control of standalone PV-hybrid system with modified IWO-based MPPT, IEEE Systems Journal, vol. 15, no. 3, pp. 3585–3596, 2020. DOI: 10.1109/JSYST.2020.3020275
6) T. Hai, D. Wang, and T. Muranaka, An improved MPPT control-based ANFIS method to maximize power tracking of PEM fuel cell system, Sustainable Energy Technologies and Assessments, vol. 54, pp. 102629, 2022. DOI: 10.1016/j.seta.2022.102629
7) T. Hai, J. Zhou, and K. Muranaka, An efficient fuzzy-logic based MPPT controller for grid-connected PV systems by farmland fertility optimization algorithm, Optik, vol. 267, pp. 169636, 2022. DOI: 10.1016/j.ijleo.2022.169636
8) P. García-Triviño et al., Power control based on particle swarm optimization of grid-connected inverter for hybrid renewable energy system, Energy Conversion and Management, vol. 91, pp. 83–92, 2015. DOI: 10.1016/j.enconman.2014.11.051
9) M. Chankaya et al., Grid-interfaced photovoltaic–battery energy storage system with slime mold optimized adaptive seamless control, IEEE Transactions on Industry Applications, vol. 58, no. 6, pp. 7728–7738, 2022, doi: 10.1109/TIA.2022.3194126.
10) A. Yasmine et al., Management of hybrid PV/battery stand-alone system under partial shading conditions, Proc. 1st Int. Conf. on Communications, Control Systems and Signal Processing, pp. 429–434, 2020. DOI: 10.1109/CCSSP49278.2020.9151784

Cite: N. Pandey, R. Pachauri, "Coati Optimization based ANFIS MPPT for PV-Battery Integrated System to Improve Power Quality". Evergreen, 13 (01) 240-255 (2026). https://doi.org/10.5109/7411064.

11) K. Srilakshmi et al., Design of soccer league optimization based hybrid controller for solar-battery integrated UPQC, IEEE Access, vol. 10, pp. 107116–107136, 2022. DOI: 10.1109/ACCESS.2022.3211504
12) E. H. Houssein et al., A modified marine predator algorithm based on opposition-based learning for tracking the global MPP of shaded PV system, Expert Systems with Applications, vol. 183, pp. 115253, 2021. DOI: 10.1016/j.eswa.2021.115253
13) N. Chettibi and A. Mellit, Intelligent control strategy for a grid connected PV/SOFC/BESS energy generation system, Energy, vol. 147, pp. 239–262, 2018. DOI: 10.1016/j.energy.2018.01.030
14) A. K. Sharma et al., Role of metaheuristic approaches for implementation of integrated MPPT-PV systems: A comprehensive study, Mathematics, vol. 11, no. 2, pp. 269, 2023. DOI: 10.3390/math11020269
15) P. Veera Manikandan and S. Selvaperumal, EANFIS-based maximum power point tracking for standalone PV system, IETE Journal of Research, vol. 68, no. 6, pp. 4218–4231, 2022. DOI: 10.1080/03772063.2020.1788425
16) S. P. Bihari and P. K. Sadhu, A novel function roach and intelligence control technique for power quality improvement in grid incorporated solar photovoltaic system, International Journal of Green Energy, vol. 19, no. 11, pp. 1170–1190, 2022. DOI: 10.1080/15435075.2021.1986403
17) A. Ramadevi et al., Optimal design and performance investigation of artificial neural network controller for solar-and battery-connected UPQC, International Journal of Energy Research, vol. 2023, pp. 3355124, 2023. DOI: 10.1155/2023/3355124
18) S. Kaur, T. Kaur, and R. Khanna, ANFIS based frequency control in an autonomous microgrid integrated with PV and battery storage, Proc. 9th Int. Conf. on Power and Energy Systems, pp. 1–4, 2019. DOI: 10.1109/ICPES47639.2019.9105593
19) H. M. Hasanien et al., Enhanced coati optimization algorithm-based optimal power flow including renewable energy uncertainties and electric vehicles, Energy, 2023. DOI: 10.1016/j.energy.2023.129069
20) M. Dehghani et al., Coati optimization algorithm: A new bio-inspired metaheuristic algorithm for solving optimization problems, Knowledge-Based Systems, vol. 259, 2023. DOI: 10.1016/j.knosys.2022.110011
21) T. Hai, A. K. Alazzawi, J. Zhou, and H. Farajian, Performance improvement of PEM fuel cell power system using fuzzy logic controller-based MPPT technique, International Journal of Hydrogen Energy, vol. 48, no. 11, pp. 4430–4445, 2023. DOI: 10.1016/j.ijhydene.2022.10.103
22) M. Dehghani, Z. Montazeri, E. Trojovská, and P. Trojovský, Coati optimization algorithm: A new bio-inspired metaheuristic algorithm for solving optimization problems, Knowledge-Based Systems, vol. 259, pp. 110011, 2023. DOI: 10.1016/j.knosys.2022.110011
23) M. Abou Houran et al., COA-CNN-LSTM: Coati optimization algorithm-based hybrid deep learning model for PV/wind power forecasting in smart grid applications, Applied Energy, vol. 349, pp. 121638, 2023. DOI: 10.1016/j.apenergy.2023.121638
24) H. M. Hasanien, I. Alsaleh, A. Alassaf, and A. Alateeq, Enhanced coati optimization algorithm-based optimal power flow including renewable energy uncertainties and electric vehicles, Energy, 2023. DOI: 10.1016/j.energy.2023.129069
25) C. H. Hussaian Basha et al., Design and implementation of hybrid MPPT controllers for solar PV systems under various partial shading conditions, Scientific Reports, vol. 14, pp. 1609, 2024. DOI: 10.1038/s41598-023-49278-9
26) C. H. Hussaian Basha et al., A universal source DC–DC boost converter for PEMFC-fed EV systems with optimization-based MPPT controller, International Transactions on Electrical Energy Systems, 2024. DOI: 10.1155/2024/5520331
27) E. Touti et al., A comprehensive performance analysis of advanced hybrid MPPT controllers for fuel cell systems, Scientific Reports 14, 12510, 2024. DOI: 10.1038/s41598-024-63074-z
28) D. Rekioua et al., Coordinated power management strategy for reliable hybridization of multi-source systems using hybrid MPPT algorithms, Scientific Reports, May 4;14(1):10267, 2024. DOI: 10.1038/s41598-024-60116-4
29) S. Rafikiran, C. H. Hussaian Basha, and C. Dhanamjayulu, A novel hybrid MPPT controller for PEMFC-fed high step-up single-switch DC–DC converter, International Transactions on Electrical Energy Systems, vol. 2024, pp. 9196747, 2024. DOI: 10.1155/2024/9196747
30) D. Rekioua et al., Coordinated power management strategy for reliable hybridization of multi-source systems using hybrid MPPT algorithms, Scientific Reports, vol. 14, pp. 10267, 2024. DOI: 10.1038/s41598-024-60116-4
31) A. M. Hussien, H. M. Hasanien, and S. F. Mekhamer, Sunflower optimization algorithm-based optimal PI control for enhancing the autonomous operation of a microgrid, Ain Shams Engineering Journal, vol. 12, no. 2, pp. 1883–1893, 2021. DOI: 10.1016/j.asej.2020.10.020
32) A. M. Hussien et al., Coot bird algorithms-based tuning PI controller for optimal microgrid autonomous operation, IEEE Access, vol. 10, pp. 6442–6458, 2022. DOI:

10.1109/ACCESS.2022.3142742

33) E. Kaymaz, S. Duman, and U. Guvenc, Optimal power flow solution with stochastic wind power using the Lévy coyote optimization algorithm, Neural Computing and Applications, vol. 33, no. 12, pp. 6775–6804, 2021. DOI: 10.1007/s00521-020-05455-9
34) M. A. M. Shaheen et al., Solution of probabilistic optimal power flow incorporating renewable energy uncertainty using a novel circle search algorithm, Energies, vol. 15, no. 21, pp. 8303, 2022. DOI: 10.3390/en15218303
35) A. Maulik, Probabilistic power management of a grid-connected microgrid considering electric vehicles, demand response, smart transformers, and soft open points, Sustainable Energy, Grids and Networks, vol. 30, pp. 100636, 2022. DOI: 10.1016/j.segan.2022.100636